

Reinfection could not occur in SARS-CoV-2 infected rhesus macaques

— [Source link](#) 

[Linlin Bao](#), [Wei Deng](#), [Hong Gao](#), [Chong Xiao](#) ...+22 more authors

Institutions: [Peking Union Medical College](#), [Capital Medical University](#)

Published on: 14 Mar 2020 - [bioRxiv](#) (Cold Spring Harbor Laboratory)

Topics: [Viral load](#)

Related papers:

- [Lack of Reinfection in Rhesus Macaques Infected with SARS-CoV-2](#)
- [Clinical features of patients infected with 2019 novel coronavirus in Wuhan, China](#)
- [A pneumonia outbreak associated with a new coronavirus of probable bat origin](#)
- [SARS-CoV-2 Cell Entry Depends on ACE2 and TMPRSS2 and Is Blocked by a Clinically Proven Protease Inhibitor](#)
- [A Novel Coronavirus from Patients with Pneumonia in China, 2019.](#)

Share this paper:    

View more about this paper here: <https://typeset.io/papers/reinfection-could-not-occur-in-sars-cov-2-infected-rhesus-6l203ht1g4>

1 **Lack of Reinfection in Rhesus Macaques Infected with SARS-CoV-2**

2

3 Linlin Bao^{†,1}, Wei Deng^{†,1}, Hong Gao^{†,1}, Chong Xiao^{†,1}, Jiayi Liu^{†,2}, Jing Xue^{†,1}, Qi
4 Lv^{†,1}, Jiangning Liu¹, Pin Yu¹, Yanfeng Xu¹, Feifei Qi¹, Yajin Qu¹, Fengdi Li¹, Zhiguang
5 Xiang¹, Haisheng Yu¹, Shuran Gong¹, Mingya Liu¹, Guanpeng Wang¹, Shunyi Wang¹,
6 Zhiqi Song¹, Ying Liu¹, Wenjie Zhao¹, Yunlin Han¹, Linna Zhao¹, Xing Liu¹, Qiang
7 Wei¹, Chuan Qin^{*,1}

8

9 ¹Beijing Key Laboratory for Animal Models of Emerging and Remerging Infectious
10 Diseases, NHC Key Laboratory of Human Disease Comparative Medicine, Institute of
11 Laboratory Animal Science, Chinese Academy of Medical Sciences and Comparative
12 Medicine Center, Peking Union Medical College, Beijing, China; ²Department of
13 Radiology, Beijing Anzhen Hospital, Capital Medical University.

14

15 [†]These authors contributed equally to this work.

16 *Correspondence should be addressed to Chuan Qin, Email: qinchuan@pumc.edu.cn.

17

18 **Abstract**

19 A global pandemic of Corona Virus Disease 2019 (COVID-19) caused by severe acute
20 respiratory syndrome CoV-2 (SARS-CoV-2) is ongoing spread. It remains unclear
21 whether the convalescing patients have a risk of reinfection. Rhesus macaques were
22 rechallenged with SARS-CoV-2 during an early recovery phase from initial infection
23 characterized by weight loss, interstitial pneumonia and systemic viral dissemination
24 mainly in respiratory and gastrointestinal tracts. The monkeys rechallenged with the
25 identical SARS-CoV-2 strain have failed to produce detectable viral dissemination,
26 clinical manifestations and histopathological changes. A notably enhanced neutralizing
27 antibody response might contribute the protection of rhesus macaques from the
28 reinfection by SARS-CoV-2. Our results indicated that primary SARS-CoV-2 infection
29 protects from subsequent reinfection.

30

31 **One Sentence Summary:**

32 Neutralizing antibodies against SARS-CoV-2 might protect rhesus macaques which
33 have undergone an initial infection from reinfection during early recovery days.

34

35 **Short Title:**

36 SARS-CoV-2-infection protect monkeys from reinfection.

37

38

39 The Corona Virus Disease 2019 (COVID-19) caused by severe acute respiratory
40 syndrome CoV-2 (SARS-CoV-2), emerged in Wuhan China, has continued to sweep
41 through Europe, America, Asia and more than millions of people have been diagnosed
42 cross the world (1, 2). Some patients discharged with undetectable SARS-CoV-2 have
43 been found re-positive during viral detection (3-5). Neutralizing antibodies (NAbs)
44 were detected 15 days posterior the onset of COVID-19 (6-8). Whether patients have a
45 risk of "relapse" or "reinfection" after recovery from initial infection have aroused the
46 worldwide concern. Therefore, in this study, we used nonhuman primates to track the
47 longitudinally infectious status from primary SARS-CoV-2 infection to reinfection by
48 the same viral strain. Seven adult Chinese-origin rhesus macaques (No M0-M6, 3-5 kg,
49 3-5-year-old) were modeled for challenge-rechallenge observation. Six monkeys (M1
50 to M6) were intratracheally challenged with SARS-CoV-2 at 1×10^6 50% tissue-culture
51 infectious doses (TCID₅₀). After they underwent mild-to-moderate COVID-19 and
52 stepped into recovering stage from the primary infection, four monkeys (M3 to M6)
53 were rechallenged intratracheally with the same dose of SARS-CoV-2 strain at 28 days
54 post initial challenge (dpi). Remained two monkeys (M1 and M2) with primary
55 infection were not rechallenged to perform as negative control of rechallenged group.
56 A healthy monkey (M0) was given an initial challenge as model control in the second
57 challenge. The pathological changes with viral-dependent distribution were compared
58 using necropsy specimens between two monkeys undergone challenge-rechallenge (M3
59 and M5) at 5 days post rechallenge (dpr, 33 dpi) and two monkeys undergone only
60 initial challenge (M0 at 5 dpi and M1 at 7 dpi). Clinical traits including body weight,
61 body temperature, chest X-ray, peripheral blood measurement, nasal/throat/anal swabs,
62 virus distribution, and pathological changes were examined at designated time points
63 (Figure 1). Weight loss ranged from 200 g to 400 g were found in four monkeys

64 undergone initial challenge (4/7) (Figure 2A), and none of monkey's rectal temperature
65 was observed elevated (0/7) (Figure 2B). Reduced appetite and/or increased respiration
66 were common (6/7) but emerged transiently with a very short time. In regard to viral
67 dissemination, peak viral load ($6.5 \log_{10}$ RNA copies/mL) was detected in nasal swabs
68 and pharyngeal swabs at 3 dpi followed with gradual decline (Figure 2C and 2D). Peak
69 viral load ($5 \log_{10}$ RNA copies/mL) could be detected using anal swabs at 3 dpi followed
70 with linearly declined to undetectable level at 14 dpi (Figure 2E). For all monkeys with
71 the initial challenge, white blood cell (WBC, $3.5\text{-}9.5 \times 10^9/\text{L}$), lymphocyte counts
72 (LYMP, $1.1\text{-}3.4 \times 10^9/\text{L}$) and neutrophil counts (NEUT, $1.8\text{-}6.4 \times 10^9/\text{L}$) fluctuated within
73 normal ranges. Comparing to the baseline, a slight yet significant reduction of WBC
74 and LYMP was observed posterior primary infection ($*p < 0.05$, Figure 2F). T
75 lymphocyte subsets including CD4^+ T cells and CD8^+ T cells maintained relatively
76 stable during the primary infectious stage (Figure 2G). Specific antibody against SARS-
77 CoV-2 was gradually increased, leading to the concentration significantly higher at 21
78 dpi compared to that at 3 dpi ($*p < 0.05$, Figure 2H). Radiologically, bilateral ground-
79 glass opacities were shown, indicating mild-to-moderate interstitial infiltration in
80 monkeys with pneumonia (Represented by M4, Figure 3A). Using necropsy specimens,
81 viral RNA copies were detected in nose (10^6 to 10^8 copies/mL), pharynx (10^4 to 10^6
82 copies/mL), lung (10^3 to 10^7 copies/mL) and gut (10^4 to 10^6 copies/mL) (Figure 3B,
83 upper panel).

84 Through HE staining, a mild to moderate interstitial pneumonia characterized by
85 widened alveolar septa, increased alveolar macrophages and lymphocytes in the
86 alveolar interstitium, and degenerated alveolar epithelia, and infiltrated inflammatory
87 cells were shown in lung from monkeys with primary infection. Amount of collagen
88 fiber could be also observed in the thickened alveolar interstitium in M0 and M1

89 monkeys by Modified Masson's Trichrome stain at 5 or 7 dpi (Figure 3C). Meanwhile,
90 the mucous membranes of trachea, tonsil, pulmonary lymph node, jejunum and colon
91 in M0 and M1 exhibited inflammatory cell infiltrations (Figure S1), and infiltration
92 with abundant CD4⁺ T cells, CD8⁺ T cells, B cells, macrophages and plasma cells in
93 lung were specified by immunohistochemistry staining (IHC) (Figure S2). The virus-
94 infected cells were mainly found in alveolar epithelia and macrophages by IHC on
95 sequential sections (Figure 3D), as well as the mucous membranes of trachea, tonsil,
96 pulmonary lymph node, jejunum and colon (Figure S1), confirming the SARS-CoV-2
97 could cause the COVID-19 in rhesus monkeys. Collectively, these data demonstrated
98 that all the seven monkeys were successfully infected with SARS-CoV-2, and the
99 characteristic of pathogenicity in monkey is similar to recent study(9-13).

100 At about 15 days posterior initial challenge, the body weight of infected monkeys
101 (M2 to M6) gradually increased into normal range (4/5, except for M4, Figure 2A). All
102 viral loads from nasopharyngeal and anal swabs returned negative (5/5, Figure 2C to
103 2E). In sera, spike protein-specific antibodies could be detected (5/5, Figure 2H, from
104 14 dpi). Chest X-ray resumed to normality at 28 dpi (5/5, Represented by M4, Figure
105 3A). These traits were similar to the discharging criteria including absence of clinical
106 symptoms, radiological abnormalities and twice negative RT-PCR negativity in human
107 infections (14). Taken together, it took about two weeks for monkeys undergone initial
108 SARS-CoV-2 stepped into recovery stage (10, 15).

109 At 28 dpi, four monkeys (M3 to M6) undergone primary infection and recovery
110 were rechallenged with the same dose of an identical SARS-CoV-2 strain
111 intratracheally. The clinical tracking of the reinfection included weight loss (Figure 2A)
112 and anal temperature (Figure 2B). A very interesting phenomenon was that the
113 rechallenged monkeys exhibited a transiently increased temperature, which was not

114 observed during the primary infection. Viral loads remained negative for a two-week
115 intensive detection using nasopharyngeal and anal swabs post rechallenge of SARS-
116 CoV-2 (Figure 2C to 2E). Peripheral blood measurements revealed no significant
117 fluctuation during the rechallenging stage (Figure 2F and 2G). Moreover, no remarked
118 abnormality of X-ray changes in M4 monkey at 33 dpi (5 dpr, Figure 3A). The only
119 notable elevation was the concentration of antibodies against SARS-CoV-2 at 42 dpi
120 (14 dpr), which is significantly higher than that at 28 dpi or 0 dpr (Figure 2H, ^{###} $p<0.01$).
121 Using necropsy specimens, there were no detectable viral RNA (Figure 3B, lower
122 panel), significant pathological lesions (Figure 3C, Figure S1), virus-infected cells
123 (Figure 3D, Figure S1) and immune cells infiltration (Figure S2) in lung and
124 extrapulmonary tissue specimens from rechallenged monkeys (M3 and M5 at 5 dpr).
125 Therefore, the rhesus monkeys with primary SARS-CoV-2 infection could not be
126 reinfected with the identical strain during their early recovering stage.

127 To interpret the challenge-rechallenge disparity, it seemed to address valuable
128 comparison of clinical, pathological and viral traits which comprehensively reflected
129 the virus-host interaction between primary challenging stage and rechallenging stage in
130 the four monkeys (M3 to M6). Firstly, viral loads from nasopharyngeal and anal swabs
131 at 5 or 7 dpi were much higher than that at 5 or 7 dpr. Secondly, increased percentage
132 of CD4⁺ T cells and decreased percentage of monocytes were observed at 7 dpr
133 compared to that at 7 dpi. Thirdly, also of the most importance, the concentration of
134 specific antibodies was much higher at 14 dpr than that at 14 dpi. The average titers of
135 neutralizing antibodies exhibited linearly increased enhancement post primary infection
136 (Table 1). Such gradually increased neutralizing antibodies against SARS-CoV-2 have
137 provided an enduring humeral immunity aroused by primary infection, which might
138 protect the same nonhuman primates from reinfection.

139 In the present challenge-rechallenge infection of SARS-CoV-2 in rhesus monkeys,
140 observation and detection were within the relative short time window that neutralizing
141 antibodies remained plateau after the primary infection. Moreover, all infected monkeys
142 affected relative mild-to-moderate pneumonia, which is similar to mild or common
143 clinical types of COVID-19 in the majority of the infected persons. Therefore, the
144 immunity of primarily infected hosts which have been mildly impaired could be
145 robustly resumed. Thirdly, mucosal immunity which have been aroused by primary
146 infection including both respiratory and intestinal mucosal and local lymph nodes might
147 contribute substantially against the newly attacked invasion of virus. A longer interval
148 (longer than 6 months) between the primary challenge and re-challenge is needed to
149 longitudinally track the host-virus interaction and elucidate the protective mechanism
150 against SARS-CoV-2 in primates.

151

152 **REFERENCE**

- 153 1. N. Zhu *et al.*, A Novel Coronavirus from Patients with Pneumonia in China, 2019. *N Engl J*
154 *Med*, 10.1056/NEJMoa2001017 (2020).
- 155 2. Coronavirus disease 2019 (COVID-19) Situation Report. *WHO*, (2020). At
156 <https://www.who.int/emergencies/diseases/novel-coronavirus-2019/situation-reports/>.
- 157 3. L. Lan *et al.*, Positive RT-PCR Test Results in Patients Recovered From COVID-19. *Jama* **323**,
158 1502-1503 (2020).
- 159 4. L. Zhou, K. Liu, H. G. Liu, Cause analysis and treatment strategies of "recurrence" with novel
160 coronavirus pneumonia (covid-19) patients after discharge from hospital. *Zhonghua jie he he*
161 *hu xi za zhi = Zhonghua jiehe he huxi zazhi = Chinese journal of tuberculosis and respiratory*
162 *diseases* **43**, E028 (2020).
- 163 5. J. An *et al.*, Clinical characteristics of the recovered COVID-19 patients with re-detectable
164 positive RNA test. *medRxiv*, 2020.2003.2026.20044222 (2020).
- 165 6. F. Wu *et al.*, Neutralizing antibody responses to SARS-CoV-2 in a COVID-19 recovered patient
166 cohort and their implications. *medRxiv*, 2020.2003.2030.20047365 (2020).
- 167 7. N. M. A. OKBA *et al.*, SARS-CoV-2 specific antibody responses in COVID-19 patients.
168 *medRxiv*, 2020.2003.2018.20038059 (2020).
- 169 8. K. K. To *et al.*, Temporal profiles of viral load in posterior oropharyngeal saliva samples and
170 serum antibody responses during infection by SARS-CoV-2: an observational cohort study. *The*
171 *Lancet. Infectious diseases*, (2020).
- 172 9. S. Lu *et al.*, Comparison of SARS-CoV-2 infections among 3 species of non-human primates.
173 *bioRxiv*, 2020.2004.2008.031807 (2020).
- 174 10. V. J. Munster *et al.*, Respiratory disease and virus shedding in rhesus macaques inoculated with
175 SARS-CoV-2. *bioRxiv*, 2020.2003.2021.001628 (2020).
- 176 11. B. Rockx *et al.*, Comparative pathogenesis of COVID-19, MERS, and SARS in a nonhuman
177 primate model. *Science*, (2020).
- 178 12. B. N. Williamson *et al.*, Clinical benefit of remdesivir in rhesus macaques infected with SARS-
179 CoV-2. *bioRxiv*, 2020.2004.2015.043166 (2020).
- 180 13. P. Yu *et al.*, Age-related rhesus macaque models of COVID-19. *Animal models and experimental*
181 *medicine* **3**, 93-97 (2020).
- 182 14. Diagnostic and treatment protocol for Novel Coronavirus Pneumonia (Trial version 6). *General*
183 *Office of National Health Commission* , (2020). At
184 <http://www.nhc.gov.cn/yzygj/s7652m/202002/54e1ad5c2aac45c19eb541799bf637e9.shtml>.
- 185 15. S. F. Wang *et al.*, Antibody-dependent SARS coronavirus infection is mediated by antibodies
186 against spike proteins. *Biochemical and biophysical research communications* **451**, 208-214
187 (2014).
- 188 16. L. Bao *et al.*, The Pathogenicity of SARS-CoV-2 in hACE2 Transgenic Mice. *bioRxiv*,
189 2020.2002.2007.939389 (2020).

190

191

192

193 **Materials and Methods**

194 *Ethics statement*

195 Seven 3- to 5-year old rhesus macaques, named as M0 to M6, were housed and cared
196 in an Association for the Assessment and Accreditation of Laboratory Animal Care
197 (AAALAC)-accredited facility. All animal procedures and experiments were carried
198 out in accordance with the protocols approved by the Institutional Animal Care and Use
199 Committee (IACUC) of the Institute of Laboratory Animal Science, Chinese Academy
200 of Medical Sciences (BLL20001). All animals were anesthetized with ketamine
201 hydrochloride (10 mg/kg) prior to sample collection, and the experiments were
202 performed in the animal biosafety level 3 (ABSL3) laboratory.

203

204 *Animal experiments*

205 For primary infection, all animals were inoculated intratracheally with SARS-CoV-2
206 (SARS-CoV-2/WH-09/human/2020/CHN isolated in our laboratory) stock virus at a
207 dosage of 10^6 TCID₅₀/1 mL inoculum volume. After the recovery, M3, M4, M5 and M6
208 were rechallenged intratracheally with the same dose (10^6 TCID₅₀/1 mL inoculum
209 volume) SARS-CoV-2 at 28 dpi. To confirm the virus distribution and pathological
210 changes, M0 at 5 dpi, M1 at 7 dpi, M3 and M5 at 33 dpi (5 dpr) were euthanasia and
211 autopsied, respectively. All animals were monitored along the timeline to record body
212 weights, body temperature, clinical signs, nasal/throat/anal swabs, hematological
213 changes, immunocytes detection, chest X-ray and specific antibody. The animal
214 experiment and longitudinal sampling schedule are shown in Figure 1.

215

216 *Quantification of SARS-CoV-2 RNA*

217 The nasal/throat/anal swab samples and mainly tissue compartments collected from

218 infected monkeys were tested for SARS-CoV-2 RNA by quantitative real-time reverse
219 transcription-PCR (qRT-PCR). Total RNA was extracted and reverse transcription was
220 performed as previously described (16). qRT-PCR reactions were carried out on an ABI
221 9700 Real-time PCR system (Applied Biosystems Instrument), the cycling protocol and
222 the primers as follows: 50°C for 2 min, 95°C for 2 min, followed by 40 cycles at 95°C
223 for 15 s and 60°C for 30 s, and then 95°C for 15 s, 60°C for 1 min, 95°C for 45 s.
224 Forward primer: 5'-TCGTTTCGGAAGAGACAGGT-3', Reverse primer: 5'-
225 GCGCAGTAAGGATGGCTAGT-3'.

226

227 *Hematology*

228 Whole blood was collected by EDTA-anticoagulation tube, and automatic hematology
229 analyzer (ProCyte Dx) was used for hematological analysis. Hematologic parameters
230 included the average total white blood cell counts (WBC), lymphocyte counts (LYPM),
231 neutrophil counts (NEUT).

232

233 *Flow cytometry*

234 Polychromatic flow cytometry was performed to analyze CD4⁺ T lymphocytes, CD8⁺
235 T lymphocytes and CD14⁺ monocytes. 50 µL of EDTA-anticoagulated whole blood
236 were stained with the monoclonal antibodies CD3 BV605 (SP34-2, BD Biosciences,
237 San Jose, CA), CD4 PerCP/Cyanine5.5 (Biolegend, 317428), CD8 FITC (Biolegend,
238 344704) and CD14 PE-Cy7 (Biolegend, 301814). The cells were resuspended in 1%
239 paraformaldehyde and subjected to flow cytometry analysis within 24 hours. All the
240 samples were analyzed by flow cytometry (FACSAria; BD, CA).

241

242 *ELISA*

243 Sera were collected from each animal for the measurement of SARS-CoV-2 antibody
244 by enzyme-linked immunosorbent assay (ELISA) along the detection timeline after the
245 initial infection. 96-well plates were coated with 0.1 µg Spike protein of SARS-CoV-2
246 (Sino Biological, 40591-V08H) overnight at 4°C and blocked with 2% BSA/PBST for
247 1 hour at room temperature. 1:100 diluted sera were added to each well and incubated
248 for 30 minutes at 37°C, followed by the HRP-labeled goat anti-monkey antibody
249 (Abcam, ab112767) incubated for 30 minutes at room temperature. The reaction was
250 developed by TMB substrate and determined at 450 nm.

251

252 *Histopathology and Immunohistochemistry*

253 Autopsies were performed according to the standard protocol in ABSL3 laboratory at
254 5 or 7 dpi for M0 and M1, 5 dpr for M3 and M5. Tissues samples were fixed in 10%
255 neutral-buffered formalin solution. Then, paraffin sections (3-4 µm in thickness) were
256 prepared and stained with Hematoxylin and Eosin (H&E) and modified Masson's
257 Trichrome stain (Masson) prior to the observation by light microscopy. For
258 immunohistochemistry (IHC) staining to identify the cell type and the expression of
259 SARS-CoV-2 antigen, paraffin dehydrated sections (3-4 µm in thickness) were treated
260 with an antigen retrieval kit (Boster, AR0022) for 1 min at 37°C and quenched for
261 endogenous peroxidases in 3% H₂O₂ in methanol for 10 min. After blocking in 1%
262 normal goat serum for 1 hour at room temperature, the sections were stained with 7D2
263 monoclonal antibody (1:500 dilution, laboratory preparation) and CD68 antibody
264 (1:500 dilution, Abcam, ab201340) at 4°C overnight, following with the incubation of
265 HRP-labeled goat anti-mouse IgG (Beijing ZSGB Biotechnology, ZDR-5307) for 1
266 hour. Alternatively, the sections were stained with CK7 antibody (1:1000 dilution,
267 Abcam, ab181598), CD4 antibody (1:500 dilution, Beijing ZSGB Biotechnology), CD8

268 antibody (1:200 dilution, Abcam, ab4055), CD20 antibody (1:500 dilution, Abcam,
269 ab78237) or CD138 antibody (1:500 dilution, Abcam, ab128936) at 4°C overnight,
270 followed by HRP-labeled goat anti-rabbit IgG secondary antibody (Beijing ZSGB
271 Biotechnology, PV9001) for 60 min. Then, the sections were visualized by incubation
272 with 3,30-diaminobenzidine tetrahydrochloride (DAB) and the image was viewed
273 under an Olympus microscope. The tissue sections (stored by our laboratory) of DMEM
274 (1 mL inoculation volume by intratracheal route)-treated monkey were used as a
275 negative control.

276

277 *Neutralizing antibody assay*

278 Sera samples were tested for the presence of neutralizing antibody observed by
279 cytopathic effect (CPE). Briefly, the sera from monkeys were heat-inactivated at 56°C
280 for 30 min. Then, serially two-fold diluted sera were incubated with 100 TCID₅₀
281 SARS-CoV-2 for 1 h at 37°C, and added into Vero-E6 cells in a 96-well-plate. Cells
282 were cultured for 1 week to observe for CPE and the serum dilution in which 50% of
283 the cells were protected from infection was calculated. Each dilution of serum was
284 tested in triplicates.

285

286 *Statistical analysis*

287 Comparisons between the two groups were determined using two-tailed unpaired
288 Student's or Welch's *t*-test. All data were analyzed with GraphPad Prism 8.0 software.

289 The level of statistical significance is designated as **p* < 0.05, ***p* < 0.01.

290

291 **ACKNOWLEDGEMENTS**

292 This work was supported by the CAMS initiative for Innovative Medicine of China

293 (Grant No. 2016-I2M-2-006), National Mega projects of China for Major Infectious
294 Diseases (Grant No. 2017ZX10304402) and National Key Research and Development
295 Project of China (Grant No. 2016YFD0500304).

296

297 **AUTHOR CONTRIBUTIONS**

298 Conceptualization: C.Q.; Methodology: L.B., W.D., H.G., C.X., J.L., J.X. and Q.L.;

299 Investigation: L.B., W.D., H.G., C.X., J.L., J.X., Q.L., J.L., P.Y., Y.X., F.Q., Y.Q., F.L.,

300 Z.X., H.Y., S.G., M.L., G.W., S.W., Z.S., Y.L., W.Z., Y.H., L.Z., X.L. and Q.W.; Writing

301 – Original Draft: J.X.; Writing –Review and Editing: J.X. and C.Q.; Funding

302 Acquisition: L.B. and C.Q.; Resources: C.Q.; Supervision: C.Q.

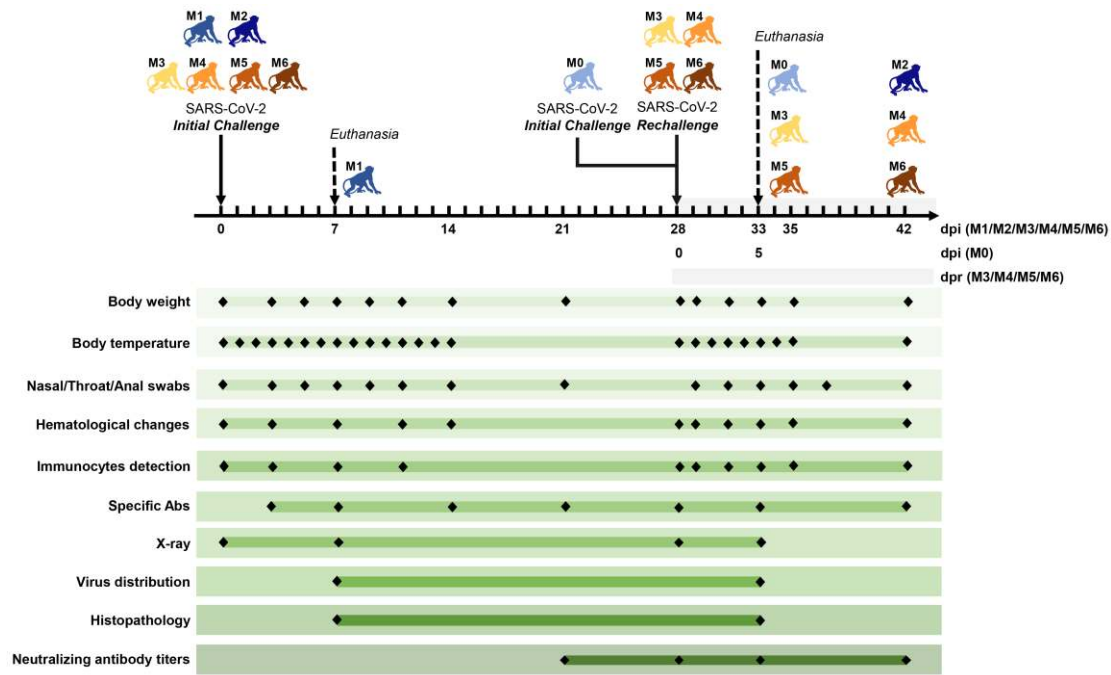
303

304 **COMPETING INTERESTS**

305 The authors have no competing interests to declare.

306

307



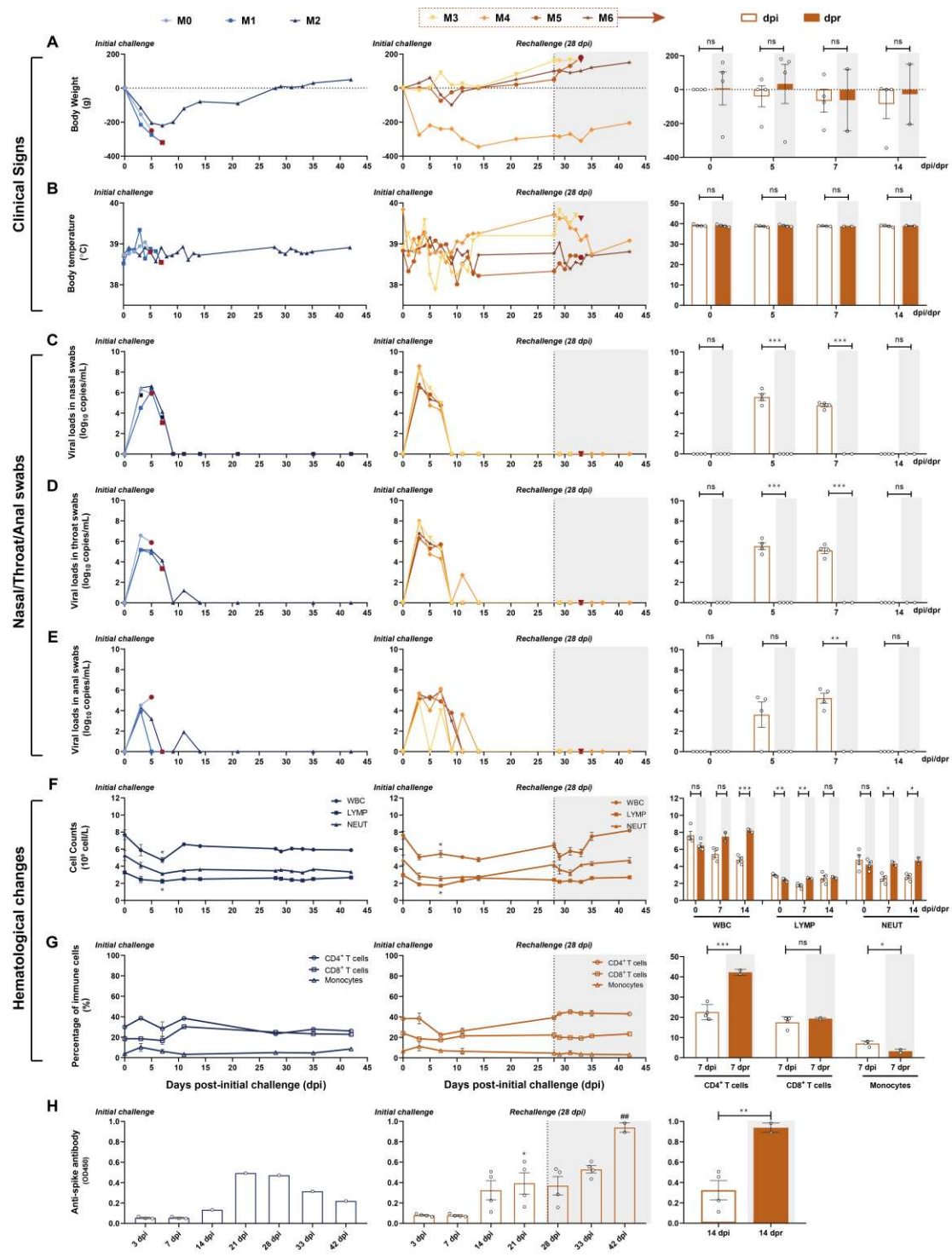
308

309 **Figure 1 Experimental design and sample collection.** Seven adult Chinese-origin
 310 rhesus macaques (M0-M6) were enrolled in current study. At the outset of this
 311 experiment, six monkeys (M1 to M6) were intratracheally challenged with SARS-CoV-
 312 2 at 1×10^6 TCID₅₀. After all the experimentally infected monkeys were recovery from
 313 the primary infection, four infected monkeys (M3 to M6) were intratracheally
 314 rechallenged at 28 days post initial challenge (dpi) with the same dose of SARS-CoV-
 315 2 strain to ascertain the possibility of reinfection. Meanwhile, uninfected monkey (M0)
 316 was also treated with SARS-CoV-2 as the model control in the second challenge, and
 317 previously infected monkey (M2) was untreated again and continuously monitored as
 318 the control. To compare the virus distribution and histopathological changes between
 319 the initially infected monkeys and the reinfected monkeys, two monkeys per group (M0
 320 and M1 in initial infection group, M3 and M5 in reinfection group) were euthanized
 321 and necropsied at 5 (M0) or 7 (M1) dpi, 5 (M3 and M5) days post rechallenge (dpr),
 322 respectively. Body weight, body temperature, nasal/throat/anal swabs, hematological
 323 changes, immunocytes and specific antibody were measured along the timeline at a
 324 short interval. Two measurements of virus distribution and histopathology (HE/IHC

325 stain) were carried out at 5 dpi (M0), 7 dpi (M1) and 5 dpr (M3 and M5). Chest X-ray
326 were detected four times and neutralizing antibody titers against SARS-CoV-2 were
327 examined at the indicated time points.

328

329



330

331 **Figure 2 Longitudinally tracking in clinical signs, viral replication, hematological**

332 **changes and immune response. (A and B) Clinical signs in each monkey. Monkeys**

333 were recorded daily for the changes in body weight and rectal temperature along the

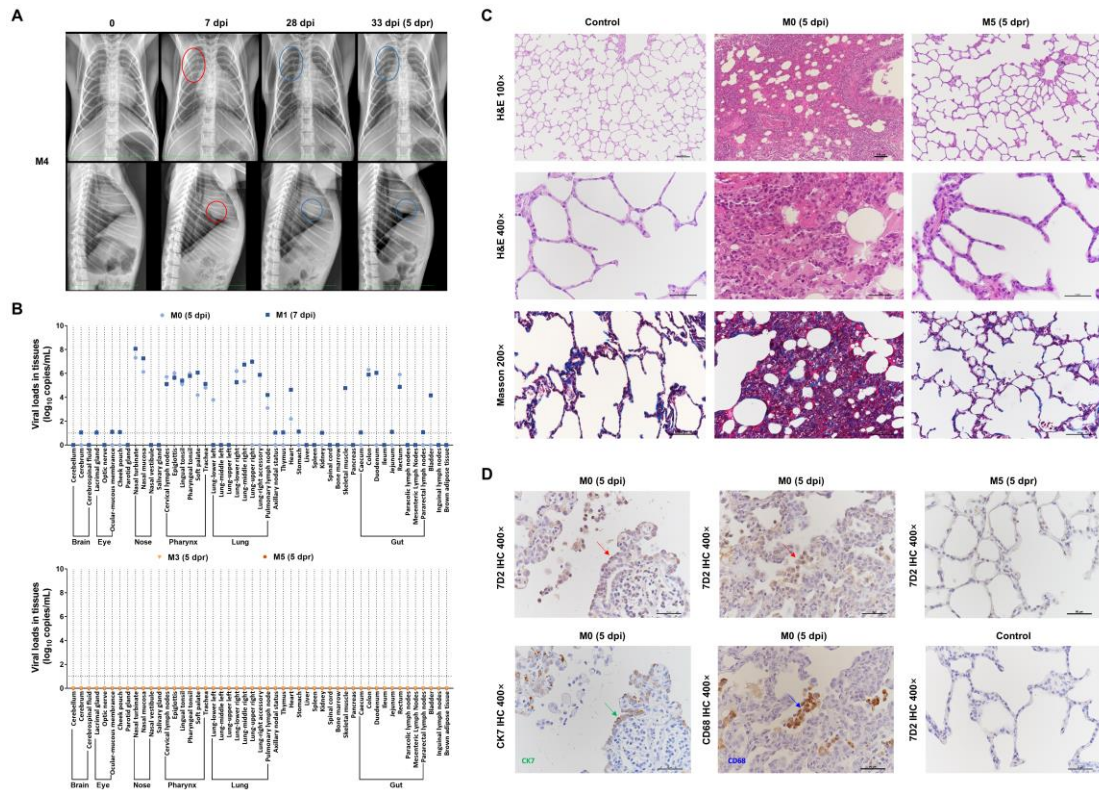
334 timeline after the initial infection followed by the virus rechallenge. The changes of

335 weights were expressed as body weight loss prior to primary infection. (C, D and E)

336 Detection of viral RNA in nasal swabs, throat swabs and anal swabs. SARS-CoV-2
337 RNA was detected by qRT-PCR in the swabs from seven monkeys at the indicated time
338 points. (F and G) Hematological changes, including cell counts of WBC, LYMP and
339 NEUT, as well as the percentage of CD4⁺ T cells, CD8⁺ T cells and monocytes in
340 peripheral blood were monitored respectively. (H) Levels of specific IgG against spike
341 protein in each monkey. The levels of anti-viral antigen specific IgG from each monkey
342 were detected at 3, 7, 14, 21, 28, 33 and 42 dpi. Four monkeys (M3-M6) were
343 rechallenged at 28 dpi (the dotted line and shaded areas), and the results of initial
344 infection and rechallenge were compared in bar graphs. The bars represented the
345 average of four rechallenged animals at the indicated time points. The viral RNA in
346 nasal, throat and anal swabs, of rechallenged animals were significantly lower than that
347 of initial infection, while the specific antibodies were significantly increased.
348 Meanwhile, significantly changes in hematological changes were observed between
349 primary and second challenge (unpaired *t*-test, **P*<0.05, ***P*<0.01; ## *P*<0.01 42 dpi
350 vs 28 dpi).

351

352



353

354 **Figure 3. Comparison of Imaging, virus distribution and pathological changes**
 355 **between primary challenge stage and rechallenge stage. (A)** Chest X ray of animals
 356 at 0, 7, 28 and 33 dpi (5 dpr) were examined and the photos of M4 was representatively
 357 shown. **(B)** Detection of viral RNA in the mainly organs, such as brain, eye, nose,
 358 pharynx, lung and gut. Compared to M0 and M1 with primary infection at 5 dpi or 7
 359 dpi, viral replication tested negatively in the indicated tissues from M3 and M5 (at 5
 360 dpr) with the virus rechallenge. Using viral load greater than 10 log₁₀ copies/mL as
 361 threshold of positivity tissue-based PCR, tissues from 49 anatomical parts were
 362 detected for qualifying virus-infected positivity. 14 tissues from respiratory tract, gut
 363 and heart were shown SARS-CoV-2 positive cells from both M0 and M1. SARS-CoV-
 364 2 positive cells were only shown in left lower lung from M0 or in right upper lung,
 365 upper accessory lung, skeletal muscle, and bladder from M1 respectively. Remained
 366 tissues from 30 anatomical parts did not find SARS-CoV-2 positive cells, indicating
 367 these tissues were intact from viral invasion. **(C and D)** In M0 (5 dpi), an interstitial

368 lesion including remarkably widened alveolar septa and massive infiltrated
369 inflammatory cells could be seen using HE staining. A mild fibrosis could be clearly
370 seen within widened alveolar septa using Masson staining. Immunohistochemistry
371 (IHC) against Spike protein of SARS-CoV-2 (7D2, red arrow), macrophage (CD68,
372 blue arrow), or alveolar epithelial cell (CK7, green arrow) were in parallel visualized
373 in Figure 3D. The Spike-positive cells overlapped with either alveolar epithelial cells
374 or macrophages have shown the diffused interstitial pneumonia affected by SARS-
375 CoV-2 invasion. In M5 (5 dpr), no remarked pathological changes and virus distribution
376 were seen via HE staining, Masson staining or IHC, indicating the interstitial lesions
377 have been completely recovered from SARS-CoV-2 primary infection and intact to
378 reinfection. 100× or 200× Black scale bar = 100 μ m. 400× Black scale bar = 50 μ m.
379 Data are representatives of three independent experiments.

380

381 Table 1 Neutralizing antibody titers to protect of SARS-CoV-2-infected Monkeys from
382 reinfection.

Animal ID	Primary challenge		Rechallenge	
	21 dpi	28 dpi	33 dpi (5 dpr)	42 dpi (14 dpr)
M0 ^a	n/a	n/a	n/a	n/a
M1 ^b	n/a	n/a	n/a	n/a
M2	1:16	1:16	1:12	1:10
M3 ^c	1:8	1:8	1:8	n/a
M4	1:16	1:16	1:40	1:160
M5 ^c	1:20	1:16	1:32	n/a
M6	1:32	1:20	1:40	1:320

383 Notes: ^a M0 was euthanized and necropsied at 5 dpi. n/a, not applicable.

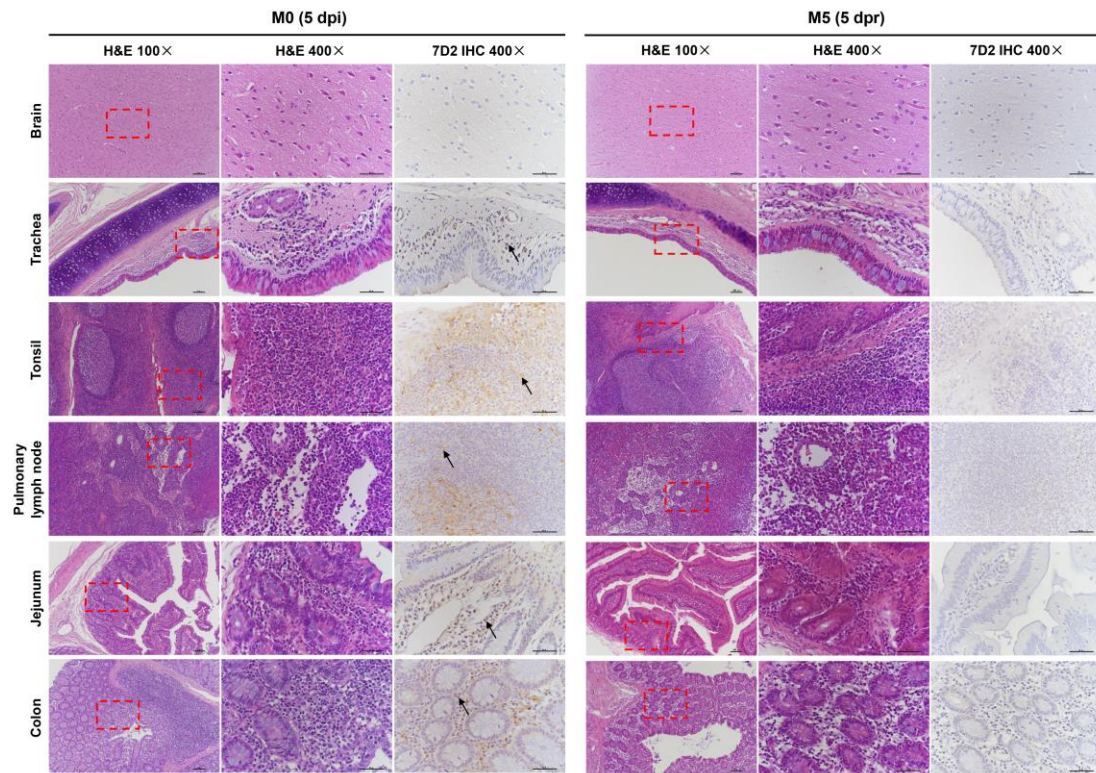
384 ^b M1 was euthanized and necropsied at 7 dpi. n/a, not applicable.

385 ^c M3 and M5 were euthanized and necropsied at 33 dpi (5 dpr). n/a, not applicable.

386

387

388

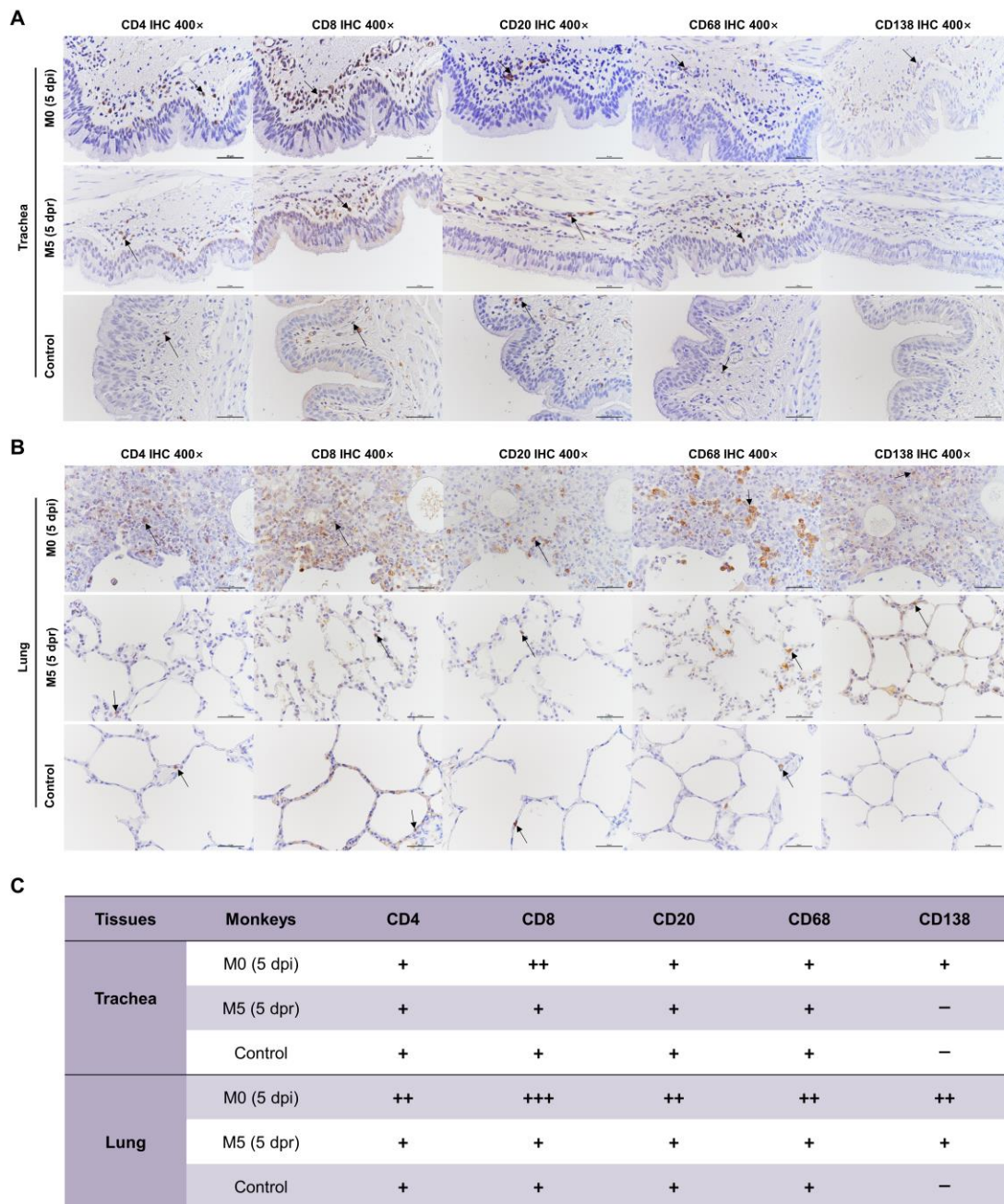


389

390 **Supplemental Figure 1. Comparison of virus distribution and pathological**
391 **changes in extrapulmonary organs between primary challenge stage and**
392 **rechallenge stage.** The pathological changes were observed by HE staining, and the
393 viral antigens were detected by Immunohistochemistry (IHC) against Spike protein of
394 SARS-CoV-2 (7D2, black arrow). In M0 (5 dpi), inflammatory cell infiltrations and
395 viral antigens were observed in mucous membranes of trachea, tonsil, pulmonary
396 lymph node, jejunum and colon, and no lesions were observed in brain. Compared to
397 M0, no remarked pathological changes and virus distribution were seen via HE staining
398 or IHC in M5 (5 dpr), indicating the animal have been completely protected from
399 rechallenge. The red frames are the area of magnification. 100× Black scale bar = 100
400 μm. 400× Black scale bar = 50 μm. Data are representatives of three independent
401 experiments.

402

403



404

405 **Supplemental Figure 2. Comparison of immune cells distribution in trachea and**

406 **lung between primary challenge stage and rechallenge stage.** The immune cells in

407 trachea (A) and lung (B) were detected by Immunohistochemistry (IHC) respectively

408 (CD4 and CD8 for T cell, CD20 for B cell, CD68 for macrophage and CD138 for

409 plasma cells), and then the number of positive cells were evaluated and scored (C).

410 Compared to control, the lung of M0 (5 dpr) was infiltrated with plenty of CD4⁺ T cell,

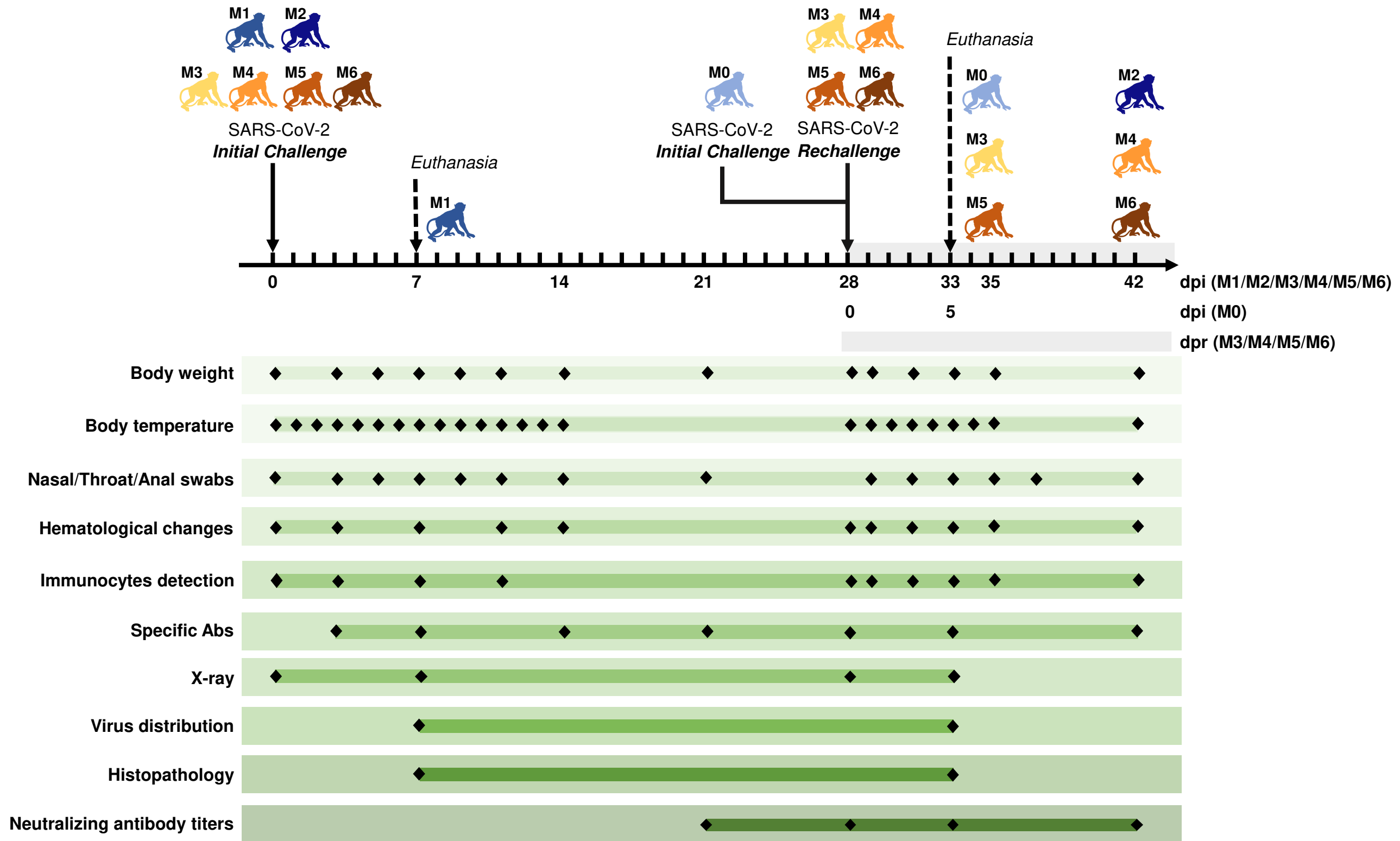
411 CD8⁺ T cell, B cells, macrophages and plasma cells, while abundant CD8⁺ T cell and

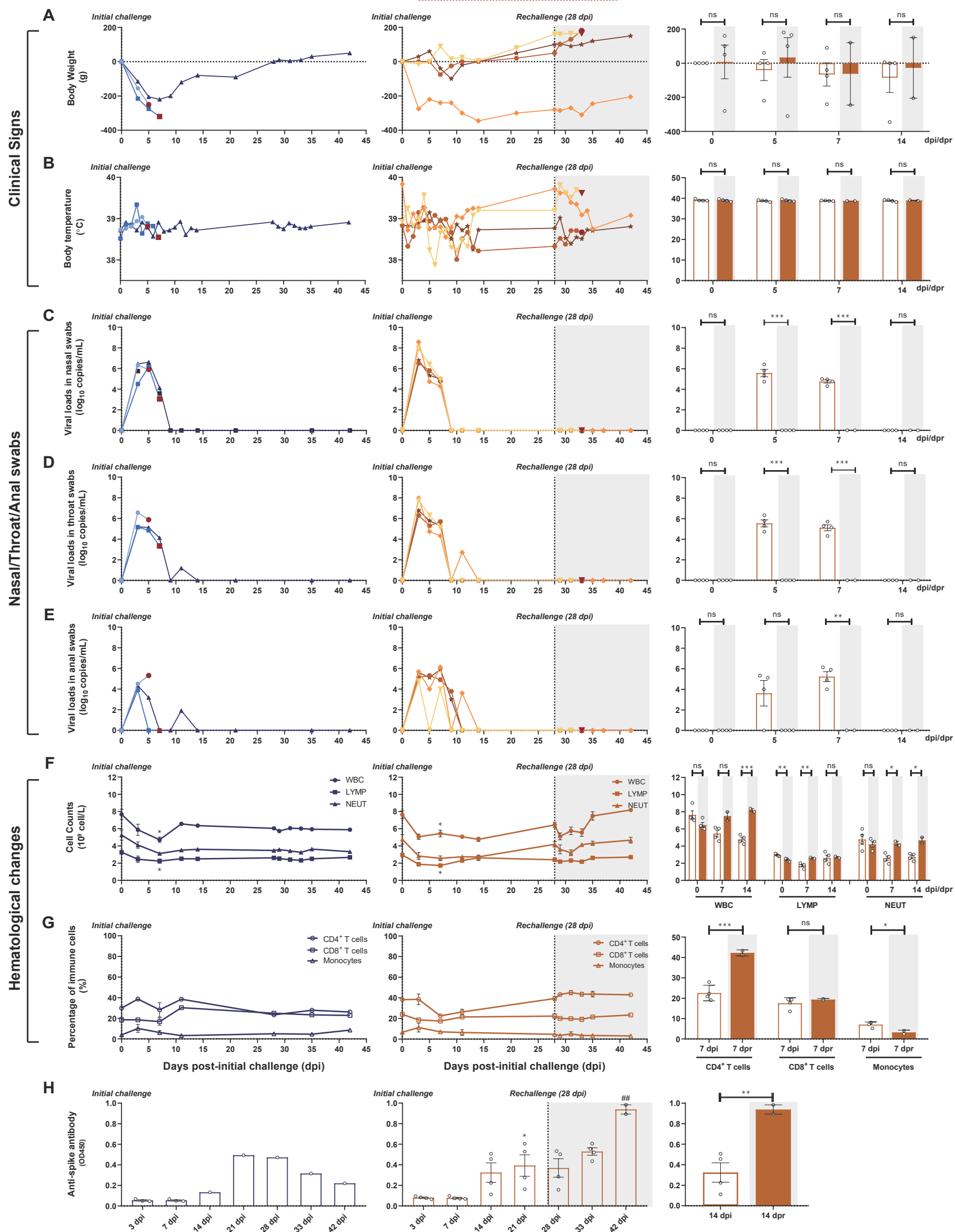
412 scattered plasma cells were also observed in trachea. No obvious difference in immune
413 cells distribution was observed in M5 (5 dpr) compared to control except the increased
414 plasma cells in lung. 400× Black scale bar = 50 μm. Data are representatives of three
415 independent experiments.

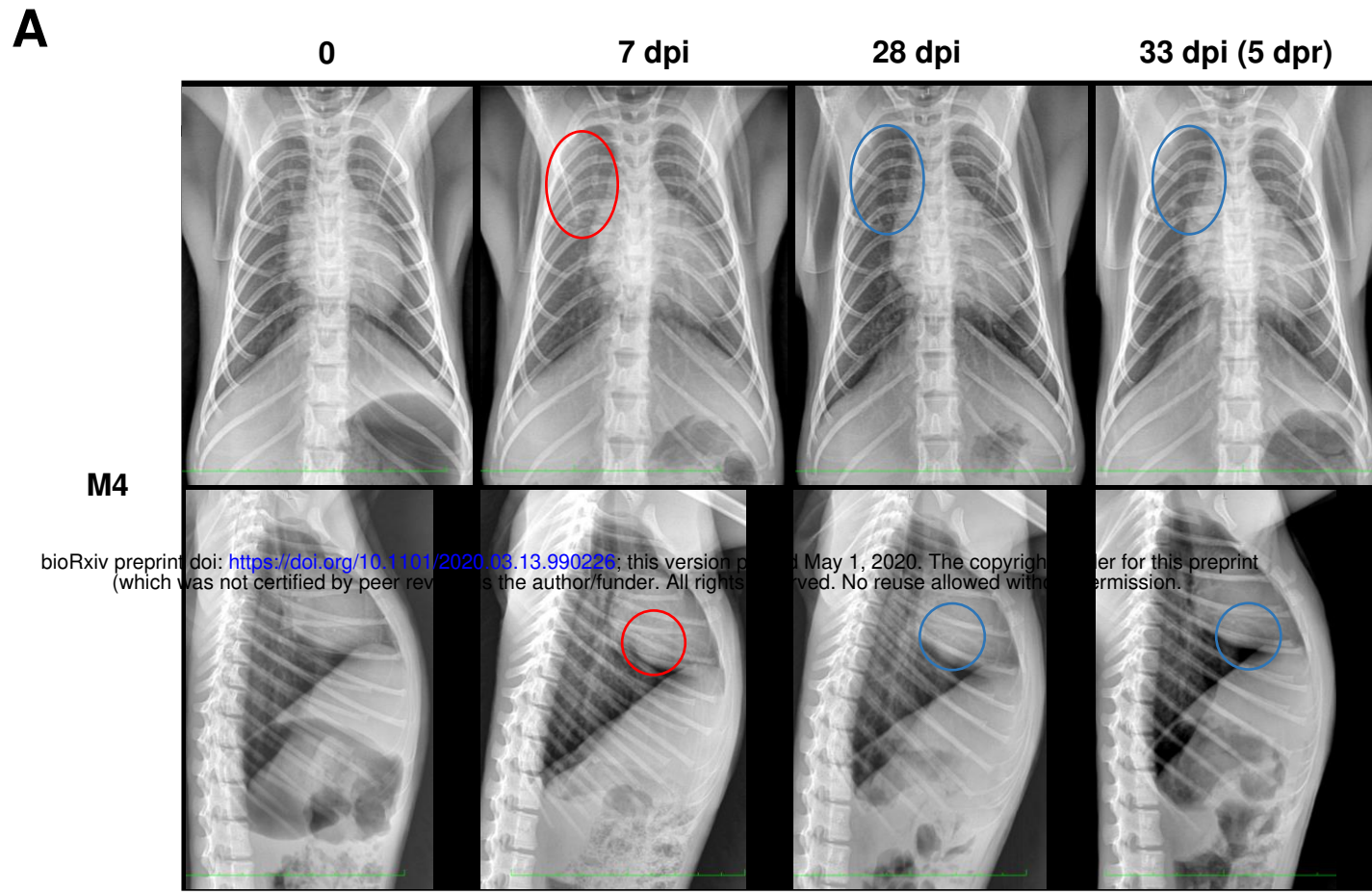
416

417

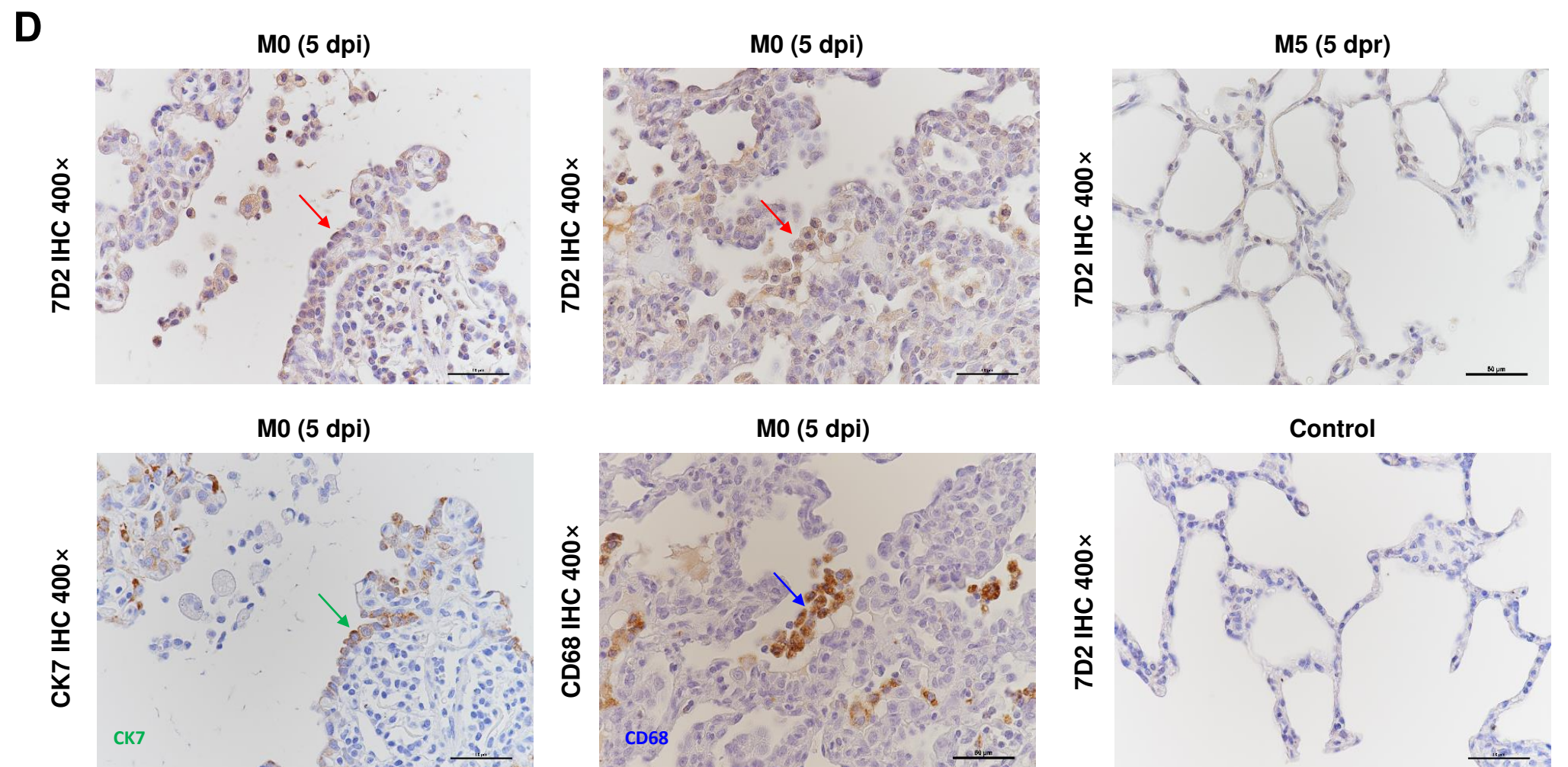
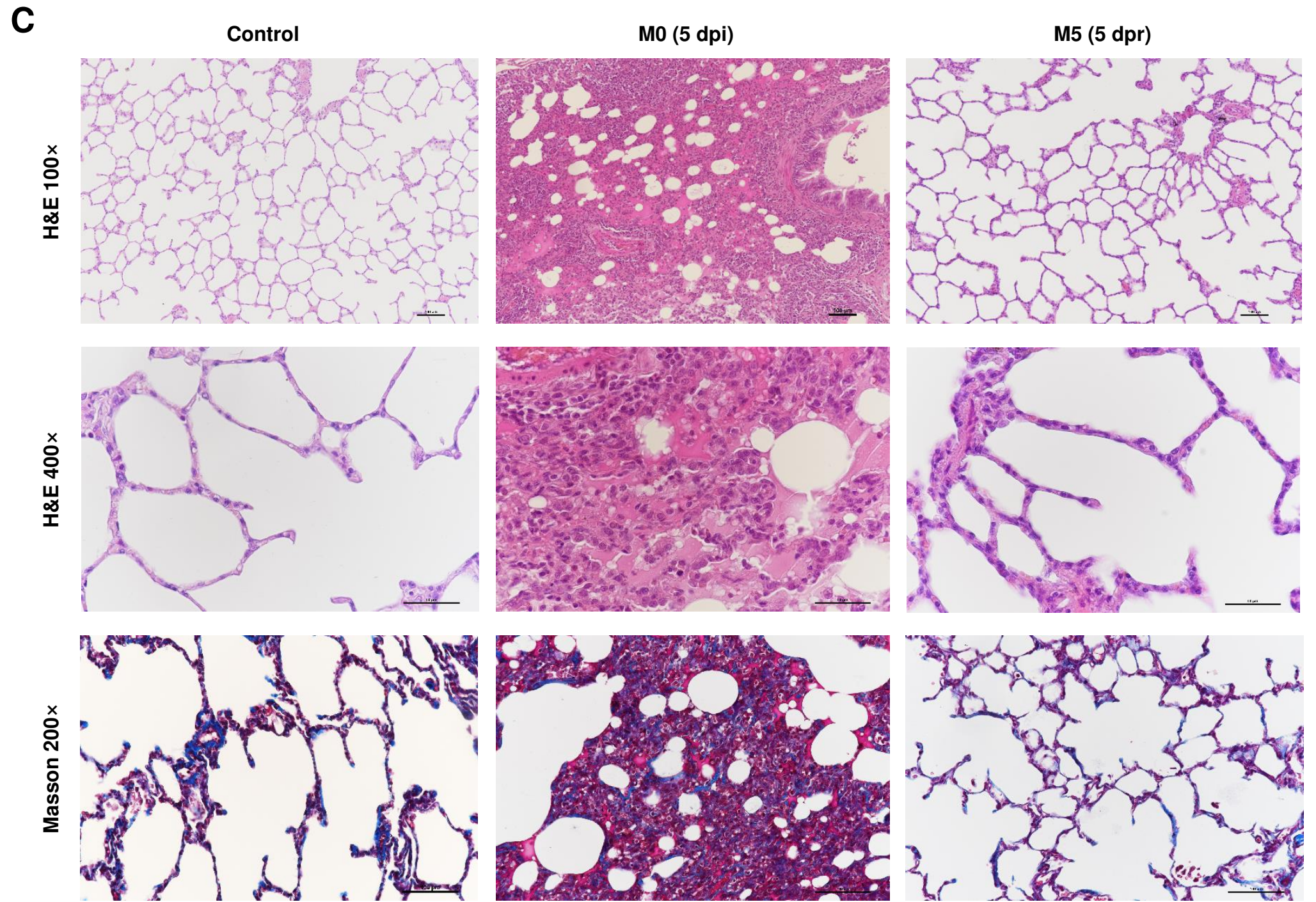
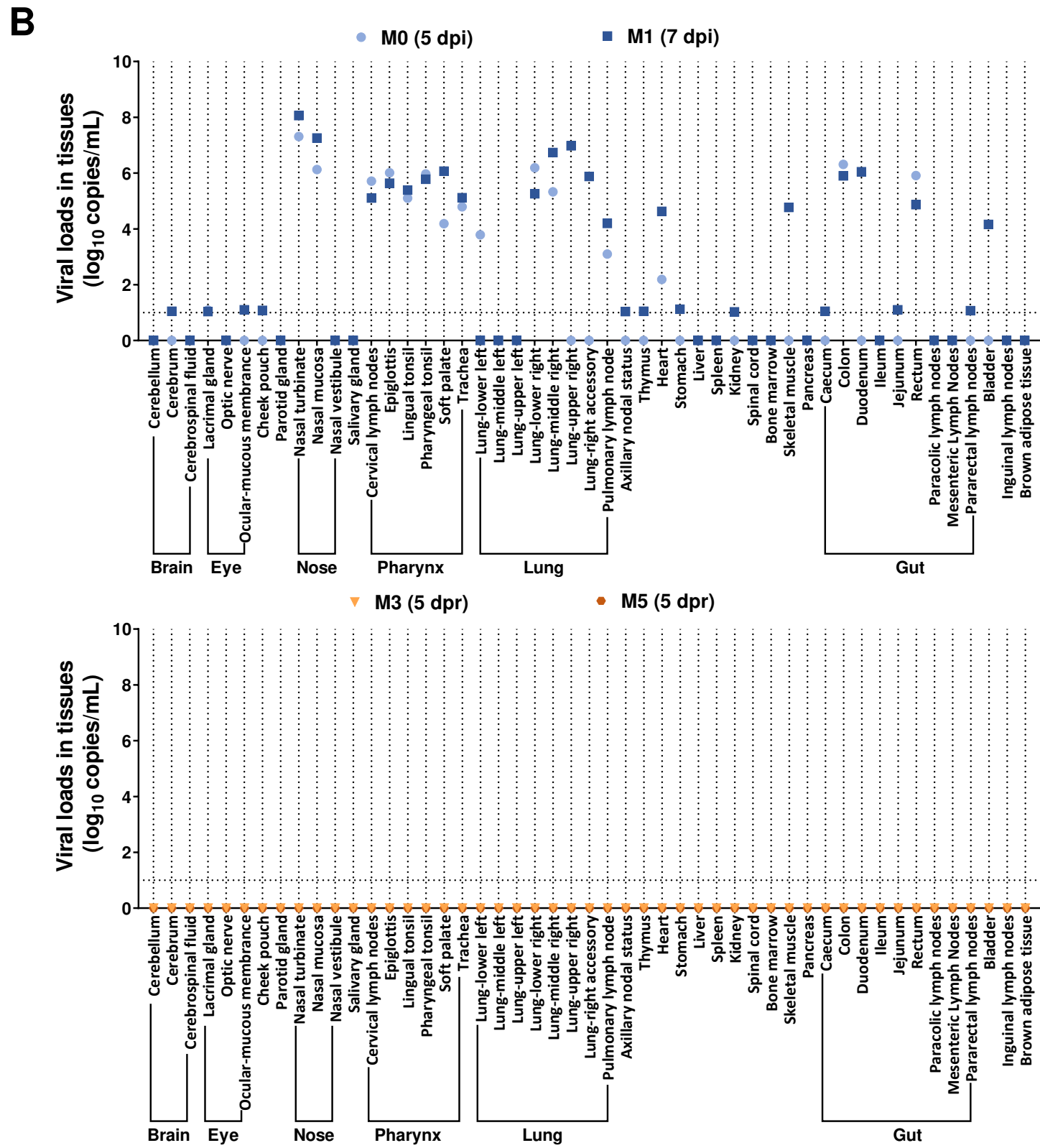
418

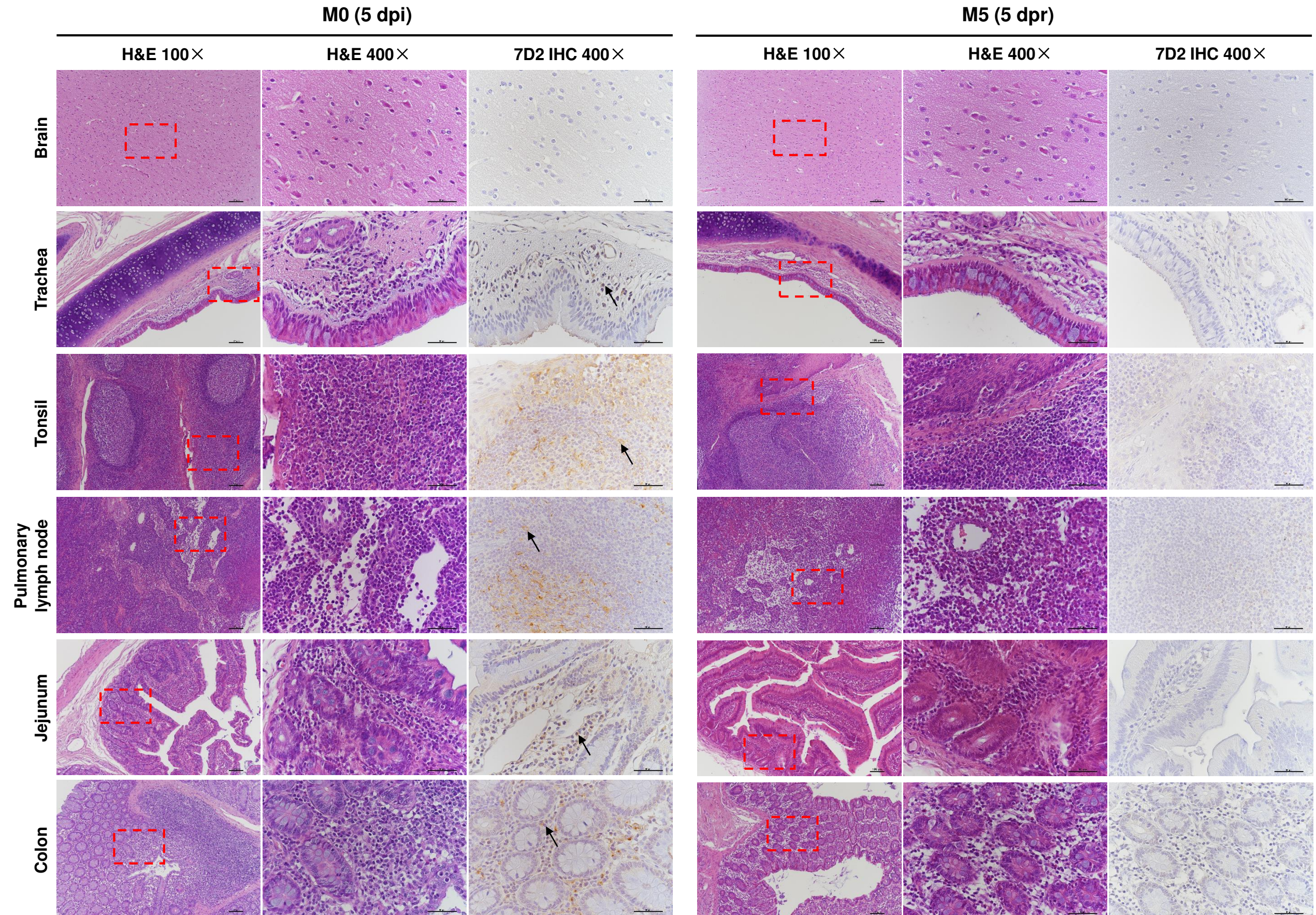


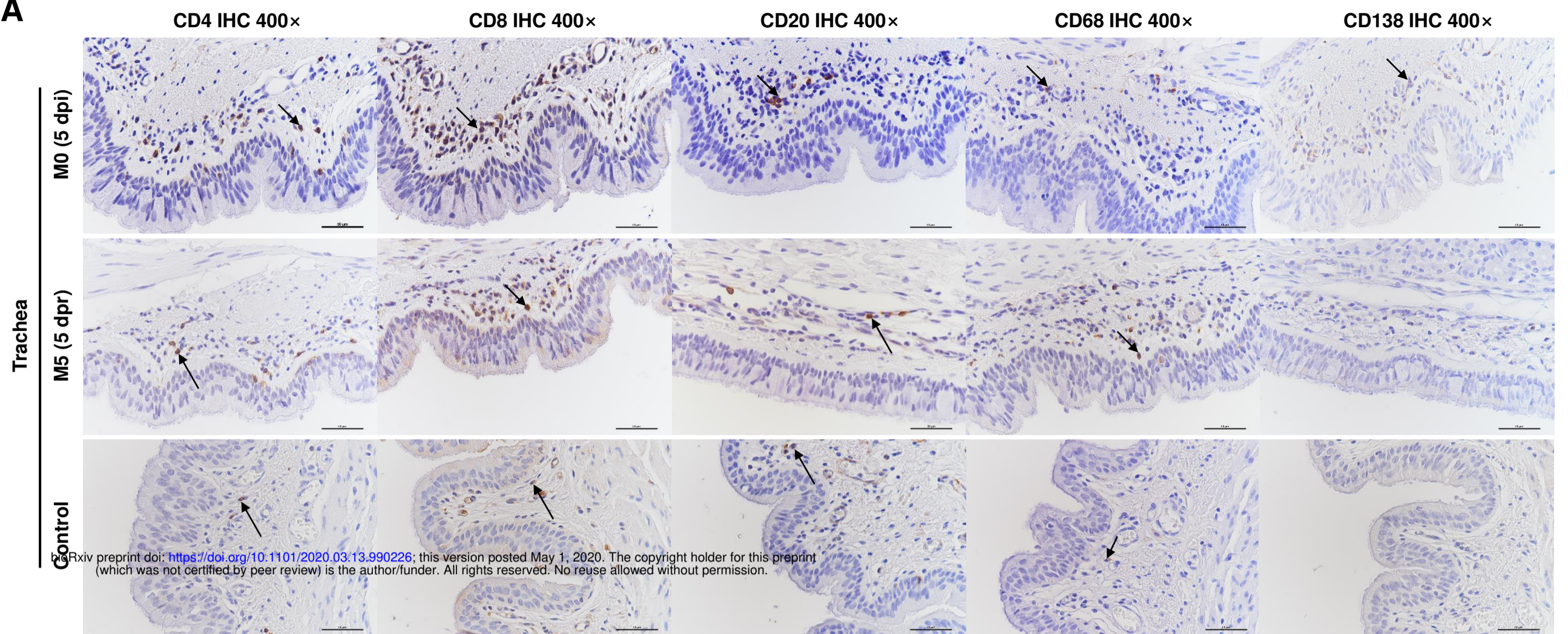
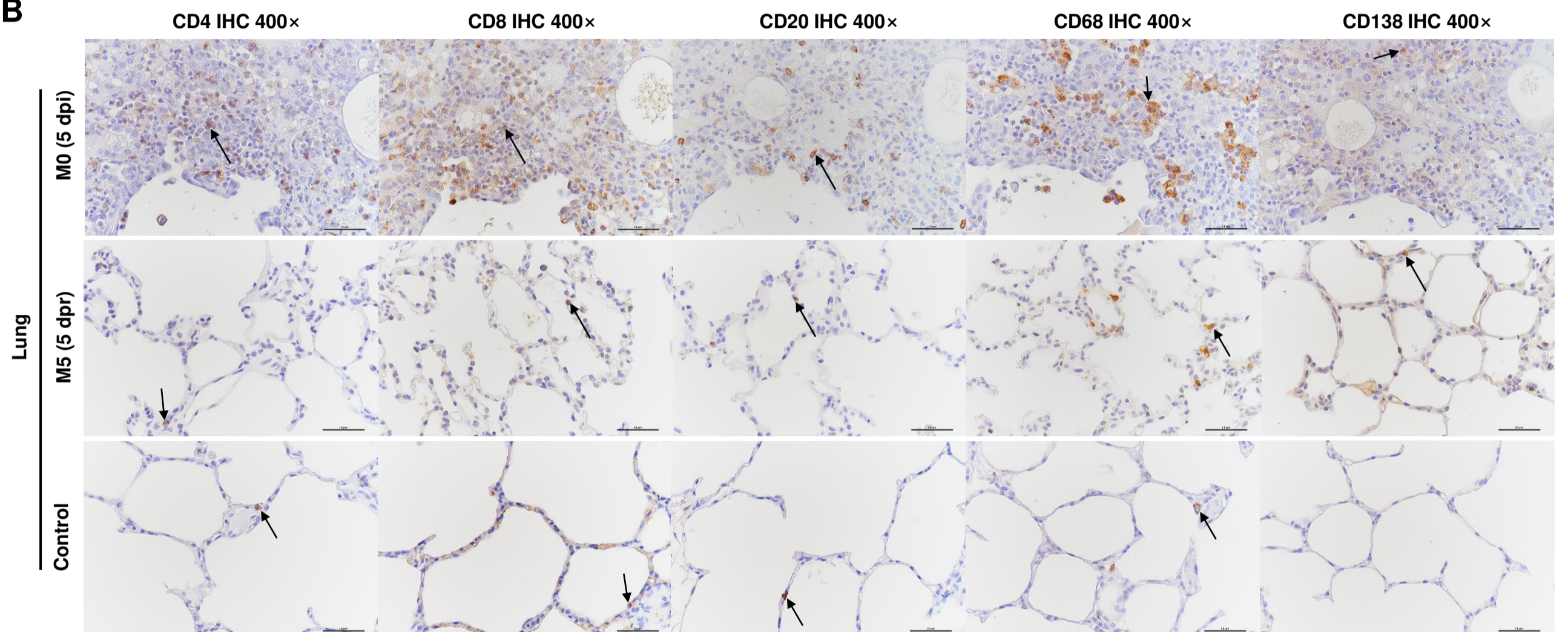




bioRxiv preprint doi: <https://doi.org/10.1101/2020.03.13.990226>; this version posted May 1, 2020. The copyright holder for this preprint (which was not certified by peer review) is the author/funder. All rights reserved. No reuse allowed without permission.





A**B****C**

Tissues	Monkeys	CD4	CD8	CD20	CD68	CD138
Trachea	M0 (5 dpi)	+	++	+	+	+
	M5 (5 dpr)	+	+	+	+	-
	Control	+	+	+	+	-
Lung	M0 (5 dpi)	++	+++	++	++	++
	M5 (5 dpr)	+	+	+	+	+
	Control	+	+	+	+	-